Cancer Science
Japanese Cancer Association JCA
Open Access

Fluorescence-lifetime molecular imaging can detect invisible peritoneal ovarian tumors in bloody ascites

Takahito Nakajima, Kohei Sano, Kazuhide Sato, Rira Watanabe, Toshiko Harada, Hirofumi Hanaoka, Peter L. Choyke and Hisataka Kobayashi

Molecular Imaging Program, Center for Cancer Research, National Cancer Institute, NIH, Bethesda, MA, USA

Key words

Fluorescence lifetime, fluorescence-guided surgery, hemorrhagic ascites, molecular imaging, ovarian cancer

Correspondence

Hisataka Kobayashi, Molecular Imaging Program, NCI/NIH, Building 10, Room B3B69, MSC 1088, Bethesda, Maryland 20892-1088, USA.
Tel: +1-301-435-4086; Fax: +1-301-402-3191;
E-mail: kobayash@mail.nih.gov

Funding information

Intramural Research Program of the National Institutes of Health, National Cancer Institute, Center for Cancer Research

Received November 18, 2013; Revised December 17, 2013; Accepted December 18, 2013

Cancer Sci **105** (2014) 308–314

doi: 10.1111/cas.12343

Blood contamination, such as bloody ascites or hemorrhages during surgery, is a potential hazard for clinical application of fluorescence imaging. In order to overcome this problem, we investigate if fluorescence-lifetime imaging helps to overcome this problem. Samples were prepared at concentrations ranging 0.3–2.4 μM and mixed with 0–10% of blood. Fluorescence intensities and lifetimes of samples were measured using a time-domain fluorescence imager. Ovarian cancer SHIN3 cells overexpressing the D-galactose receptor were injected into the peritoneal cavity 2.5 weeks before the experiments. Galactosyl serum albumin-rhodamine green (GSA-RhodG), which bound to the D-galactose receptor and was internalized thereafter, was administered intraperitoneally to peritoneal ovarian cancer-bearing mice with various degrees of bloody ascites. *In vitro* study showed a linear correlation between fluorescence intensity and probe concentration ($r^2 > 0.99$), whereas the fluorescence lifetime was consistent (range, 3.33 ± 0.15–3.75 ± 0.04 ns). By adding 10% of blood to samples, fluorescence intensities decreased to <1%, while fluorescence lifetimes were consistent. *In vivo* fluorescence lifetime of GSA-RhodG stained tumors was longer than the autofluorescence lifetime (threshold, 2.87 ns). Tumor lesions under hemorrhagic peritonitis were not depicted using fluorescence intensity imaging; however, fluorescence-lifetime imaging clearly detected tumor lesions by prolonged lifetimes. In conclusion, fluorescence-lifetime imaging with GSA-RhodG depicted ovarian cancer lesions, which were invisible in intensity images, in hemorrhagic ascites.

Fluorescence imaging is increasingly being used as an aid to surgery for such indications as detection of sentinel lymph nodes in cancer patients,[1–3] determining tissue perfusion of skin flaps [4–8] and demonstrating lymphatic stasis and leakage.[9,10] One particularly promising application is the use of fluorescence imaging for detecting tiny cancers that might be concealed by complex anatomy, such as that found in the peritoneum where the bowel and omentum create multiple creases in which micrometastases can hide. Using fluorescent conjugates that bind to the tumors with high affinity but wash off normal peritoneal surfaces, dramatically more lesions can be identified and removed by the surgeon, decreasing the likelihood of recurrence. Unlike probes elsewhere in the body, where depth of light penetration is important and therefore near infrared emitters are preferred, detection of peritoneal lesions can be accomplished with green light emitters, which have the advantages that they can be easily seen with the naked eye, which is optimized for green light, and are chemically smaller than near-infrared emitting probes and therefore possess superior pharmacokinetics.

Intraoperative fluorescence imaging has, to date, focused on simply detecting a fluorescence signal from the tumor. Unfortunately, in the case of peritoneal metastases, it is difficult to completely eliminate pools of fluid, particularly bloody ascites, which can dramatically reduce the detectable fluorescence. However, another property of fluorescence, fluorescence lifetime (FLT), is potentially less susceptible to such effects.[11–14] For instance, fluorescence-lifetime imaging microscopy (FLIM) has recently been used to refine the imaging of intracellular microstructure wherein only very small amounts of fluorescence intensity can be detected.[15–17] The FLIM can detect changes within microenvironments independent of fluorescence intensities and power of excitation lights with excellent signal-to-noise characteristics because background lifetimes are considerably different than lifetimes associated with internalized fluorophores. Fluorescence lifetimes are altered by the chemical environments, in which the fluorophores are found and have relatively better signal-to-noise ratios than fluorescence alone, which must compete against background autofluorescence that often overlaps with the target fluorophore's emission spectrum.

Because green light is well absorbed and scattered by red blood cells containing hemoglobin, even small amounts of blood severely compromise the fluorescence intensity of green fluorescent probes. During surgical or endoscopic procedures, it is not uncommon for blood to contaminate the imaging field of view. Therefore, hemorrhage is an important obstacle for fluorescence imaging. Because FLT is independent of fluorescence intensity, it has the potential to address this issue.

In the present study, we use a green fluorescent probe, galactosyl serum albumin-rhodamine green (GSA-RhodG), in

an animal model of ovarian cancer with peritoneal metastases to define the advantages of FLT imaging (FLTI) over fluorescence intensity imaging (FII) when overcoming the problem of blood contamination within the peritoneum during surgery.

Materials and Methods

Reagents. Galactosyl serum albumin was purchased from Sigma Chemical (St. Louis, MO, USA) and amino-reactive Rhodamine Green (RhodG-NHS) was purchased from Invitrogen Corporation (Carlsbad, CA, USA).

Cells. A D-galactose receptor-positive ovarian cancer cell line, SHIN3, was used in the present study. Cells were grown in RPMI1640 supplemented with 10% fetal bovine serum and 1% penicillin/streptomycin in tissue culture flasks in a humidified incubator at 37°C in an atmosphere of 95% air and 5% carbon dioxide.

Synthesis of RhodG-conjugated GSA. At room temperature, 1 mg (14 nmol) of GSA in 0.1 M Na_2HPO_4 was incubated with 70.1 nmol of RhodG-NHS at pH 8.5 for 30 min. The mixture was purified with a gel filtration column (Sephadex G50 column, PD-10; GE Healthcare, Piscataway, NJ, USA) and the GSA binding fraction (2.6–3.8 mL) was eluted by 0.066 M PBS at pH 7.4 and collected in a test tube. GSA-RhodG was kept at 4°C in the refrigerator as a stock solution.[18] The protein concentrations of GSA-RhodG samples were determined using the Coomassie Plus protein assay kit (Pierce Biotechnology, Rockford, IL, USA) by measuring the absorption at 595 nm with a UV-Vis system (8453 Value UV-Visible Value System; Agilent Technologies, Santa Clara, CA, USA) using standard solutions of known concentrations of GSA (100 μg/mL). The concentration of RhodG was then measured by absorption at 503 nm with the UV-Vis system to confirm the number of fluorophore molecules conjugated to each GSA molecule. The number of fluorophore molecules per GSA was adjusted to approximately two.

Animal model of ovarian cancer peritoneal metastases. All procedures were carried out in compliance with the Guide for the Care and Use of Laboratory Animal Resources (1996), National Research Council, and approved by the local Animal Care and Use Committee.

Intraperitoneal tumor xenografts were established by intraperitoneal injection of 2×10^6 SHIN3 cells suspended in 300 μL of PBS in female nude mice (National Cancer Institute Animal Production Facility, Frederick, MD, USA). Imaging of tumor-bearing mice was performed at 14–21 days after injection of the cells.

Fluorescence-lifetime measurements. All FLT experiments were conducted with the eXplore Optix-MX2 system (ART Advanced Research Technologies, Inc., Montreal, Canada). A fixed pulsed laser diode (70 ps) was used as an excitation source at a wavelength of 470 nm. Fluorescence data were acquired using a bandpass filter from 500 to 550 nm for emission light. Region of interest (ROI) measurements with a spot size of 1.5 mm were selected at the image plane. The laser power and duration were automatically chosen as the highest power that does not saturate the photon detector. Lifetime analysis was performed with commercial software (ART OptiView; ART Advanced Research Technologies, Inc.). Lifetime values and lifetime mapping were calculated to fit fluorescence temporal point-spread functions (TPSF) as single-exponential models with the Fit TPSF tool. Briefly, using the automatic mode of the Fit TPSF tool, the program automatically selected the second (slower) part of the decay curve and then fitted a single exponential model and calculated the fluorescence lifetime, as shown in Figure 1. The software also provides a curve fitting range and error rate when calculating FLT (Fig. 1c). If the curve-fitting range was appropriate and the error stayed within the threshold, we accepted the FLT value. In cases where the error was greater than the threshold due to mixed FLT values, we used dual- or multiple-exponential modes with manual selection of curve ranges, although this rarely happened in the present study. In general, the FLT of autofluorescence was shorter than 1.8 ns (Fig. 1b), which was much shorter than RhodG FLT (longer than 3.3 ns). Therefore, this large difference of FLT allowed the automatic mode to detect

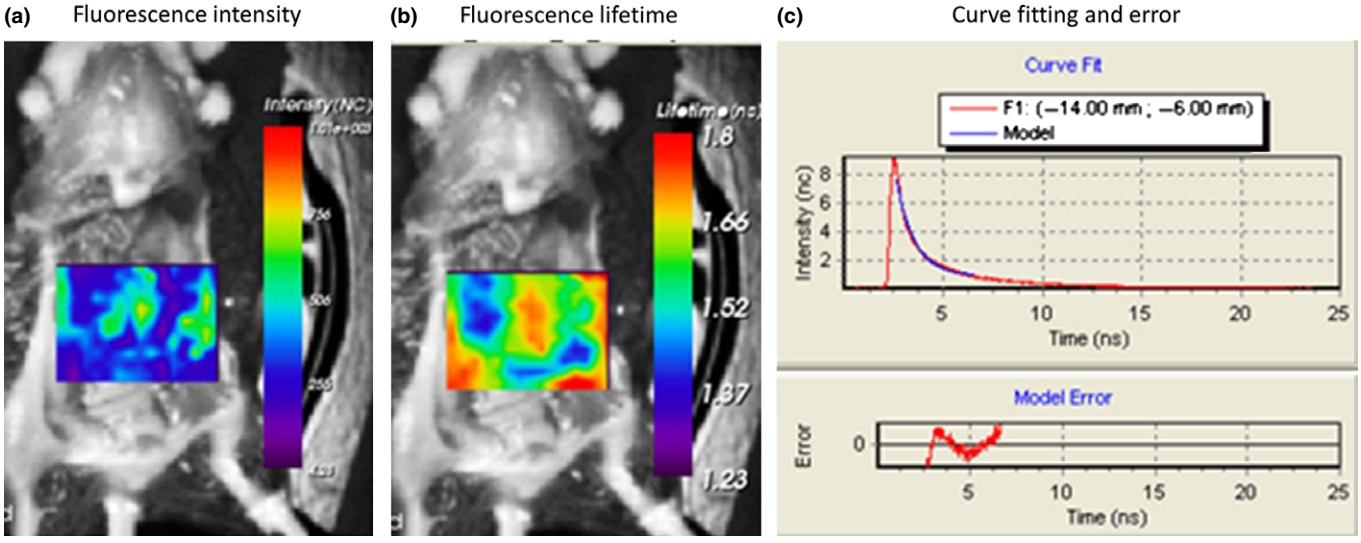

Fig. 1. Autofluorescence fluorescence intensity (a) and fluorescence-lifetime (b) images of a mouse abdomen are shown with graphs of fluorescence decay, curve fitting and model error (c) using the Fit TPSF tool. Autofluorescence fluorescence lifetime in the mouse abdomen was consistently shorter than 1.8 ns, which was much shorter than rhodamine green (3.3 ns).

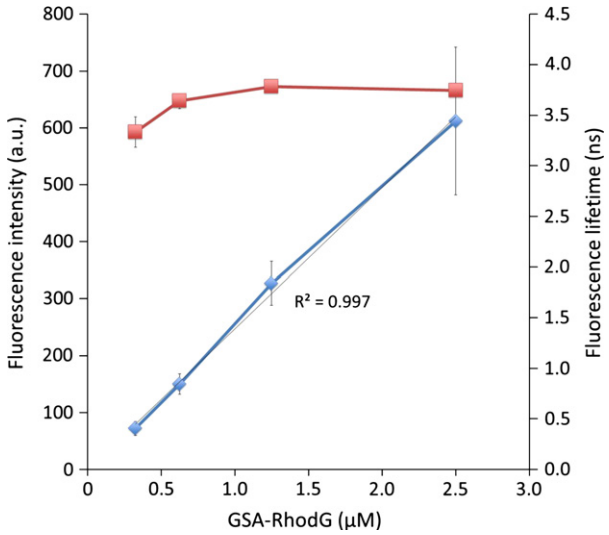

Fig. 2. Relationship between the fluorescence intensity and the fluorescence lifetimes (FLT) of galactosyl serum albumin-rhodamine green (GSA-RhodG) at various concentrations. The values of relative fluorescence intensities of GSA-RhodG solution (blue line) were measured and plotted on the *y*-axis against the concentration of GSA-RhodG on the *x*-axis. At the same time, the FLT (red line) was calculated and plotted on the same graph. Fluorescence intensities were proportional to the concentration of solutions whereas FLT values were completely independent of the concentration.

RhodG FLT without fail, provided that the RhodG signal was sufficient for detection.

***In vitro* FLTI studies.** The GSA-RhodG solutions were prepared at concentrations of 20.8, 41.7, 83.3 and 166.7 μg/mL (0.3, 0.6, 1.2 and 2.4 μM) and plated in 1.7 mL centrifuge tubes. The fluorescence intensities and lifetimes of each sample were obtained using the Optix-MX2 system.

SHIN3 cells were plated on 75 mm^2 cell culture flasks and incubated until confluent. Then, GSA-RhodG conjugate was added to the media at a final concentration of 1 μg/mL and cells were incubated for 1 and 6 h at 37°C. On completion of incubation, cells were removed from the flasks and centrifuged to obtain pellets. The resulting cell pellets were washed twice with PBS and placed in 1.7 mL centrifuge tubes. The fluorescence intensities and lifetimes of each sample were obtained.

To investigate the effect of blood contamination with GSA-RhodG solution, murine blood collected from a mouse by direct puncture of the heart was added to the GSA-RhodG solutions at concentrations of 2.5%, 5% and 10%. Then, FLT and fluorescence intensity measurements of each sample were acquired and the data were compared with the control GSA-RhodG solution without blood.

***In vivo* FLTI compared with FII.** Twenty-five micrograms GSA-RhodG were diluted in 300 μL PBS (83.3 μg/mL) and injected into the peritoneal cavities of mice with peritoneally disseminated cancer implants. One hour after intraperitoneal injection, mice were killed using carbon dioxide inhalation. Immediately after euthanasia, the abdominal cavity was exposed and the mice were placed on a non-fluorescent plate to compare the fluorescence intensity of the tumors. Spectral fluorescence images were obtained using the Maestro In-Vivo Imaging System (CRi Inc., Woburn, MA, USA). A bandpass blue filter from 445 to 490 nm and a long pass filter over 515 nm were used for excitation and emission light, respectively. The tunable filter was automatically stepped in 10-nm increments from 500 to 800 nm while the camera captured images at each wavelength interval with constant exposure. To compare with the FLTI acquired using the Optix-MX2 system, non-stepped images were obtained using a filter between 540 and 550 nm. The FLTI and FII of the same mice were then acquired using the Optix-MX2 system under the following conditions: pulse excitation wavelength, 470 nm; and emission filter, 500–550 nm. The ROI measurements with a diameter of 1.5 mm were selected at the image plane. A single session of FLTI and FII took approximately 7 min. Maestro images were used to identify the implantation sites of tumor within the peritoneal cavity. According to this definition, the tumors and normal tissue were distinguished on both FLTI and FII. Additionally, a "dot by dot" comparison between FLT values and fluorescence intensities were recorded using the Optix-MX2 system.

Fluorescence-lifetime images with bloody ascites. Peritoneal ovarian cancer implants were harvested with various degrees of hemorrhagic ascites 14 days after intraperitoneal injection of SHIN3 cells. Mice were imaged with ascites (~0%, ~2.5%, ~5.0% and ~10% blood) partly covering the peritoneal tumors. The fluorescence intensity measurements were acquired using both Maestro and Optix-MX2 and the FLTI were obtained with the Optix-MX2. All tumors detected using FLTI were confirmed by histological analysis.

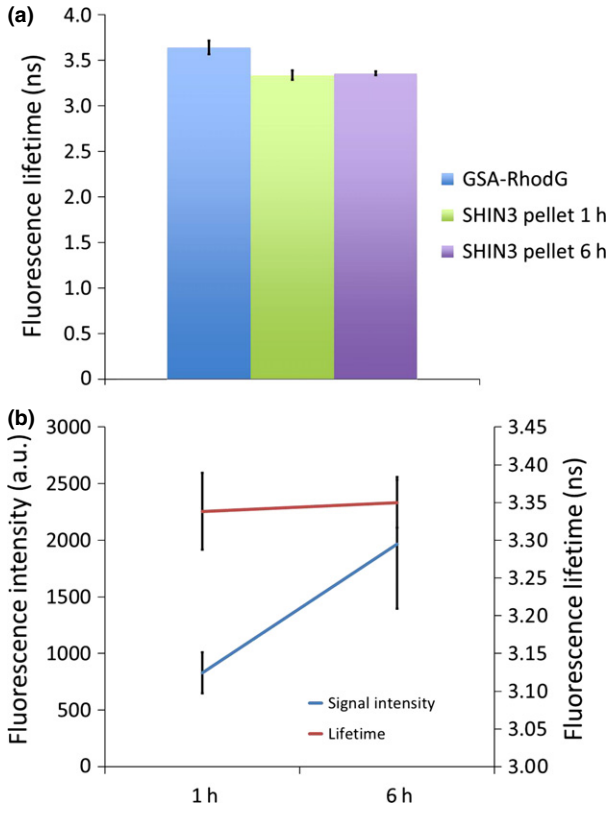

Fig. 3. Comparison of fluorescence lifetime for galactosyl serum albumin-rhodamine green (GSA-RhodG) solution and SHIN3 pellets incubated with GSA-RhodG. (a) The fluorescence lifetime of GSA-RhodG solution (25 μg/300 μL) was compared with the pellets of SHIN3 cells incubated with GSA-RhodG at a concentration of 10 μg/mL for 1 h or 6 h. (b) The relationship between the fluorescence intensity and the lifetime of SHIN3 pellets incubated for 1 h and 6 h. While there was no difference in fluorescence lifetime of cell pellets incubated for 1 h and 6 h ($P = 0.12$), the fluorescence intensities demonstrated significant differences between 1 h and 6 h ($P < 0.05$).

Statistical analysis. Data are expressed as mean ± SEM. Statistical analyses were carried out using the Student's *t*-test (Prism6; GraphPad Software Inc., La Jolla, CA, USA).

Results

Fluorescence lifetime of GSA-RhodG is consistent regardless of the concentration. The fluorescence intensities of GSA-RhodG solutions showed a positive linear correlation with concentration in the range 0.3–2.4 μM ($r^2 > 0.99$). In contrast, the FLT in the same concentration range was approximately constant (range, 3.33 ± 0.15–3.75 ± 0.04 ns; Fig. 2).

SHIN3 pellets incubated with GSA-RhodG (10 μg/mL) also showed that FLT after 1 h incubation were identical to those after 6 h incubation (1 h, 3.34 ± 0.05 ns; 6 h, 3.36 ± 0.03 ns); however, fluorescence intensities increased with incubation time (1 h, 831 ± 180 a.u.; 6 h, 1966 ± 569 a.u.; Fig. 3b). The GSA-RhodG solution by itself (concentration 25 μg/300 μL or 1.2 μM) had a similar but slightly longer FLT than SHIN3 pellets incubated with GSA-RhodG (3.64 ± 0.24 ns *vs* 3.34 ± 0.05 ns; Fig. 3a).

Mixture with whole blood decreases fluorescence intensity but does not affect FLT. When adding 2.5% of whole mouse blood to the GSA-RhodG solution, fluorescence intensities of GSA-RhodG solutions at various concentrations (20.8, 41.7 and 83.3 μg/mL) decreased to 3.45 ± 0.75%, 4.86 ± 0.25% and 11.46 ± 1.53%, respectively (Fig. 4). When adding 10% of blood to the GSA-RhodG solution, fluorescence intensities decreased to <1% (Fig. 4a). However, FLT of GSA-RhodG solutions at all concentrations examined were consistent before and after adding various concentrations (2.5%, 5% and 10%) of whole blood (Fig. 4b).

Fluorescence lifetime of tumor containing GSA-RhodG is longer than autofluorescence lifetime *in vivo*. The tissue harboring SHIN3 tumors (Fig. 5a, blue rectangle) showed a significantly higher fluorescence intensity and longer FLT than the normal peritoneum (Fig. 5a, red rectangle) ($P = 0.0002$ and $P < 0.0001$, respectively; Fig. 5a,b). The FLT of voxels containing SHIN3 tumors were mostly longer than 2.87 ns; however, autofluorescence lifetimes in non-tumor areas were <2.87 ns (Fig. 5c).

Fluorescence-lifetime imaging depicts ovarian cancer implants with hemorrhagic ascites. Mild hemorrhagic ascites compromised tumor-to-background contrast on fluorescence intensity images. In mice with moderate and severe hemorrhagic ascites, tumors were undetectable on fluorescence intensity images. However, FLTI depicted tumors by their prolonged FLT despite the presence of bloody ascites insofar as some fluorescence signal was detectable up to a limit of approximately 10% blood (Fig. 6). All tumor lesions were confirmed using histological analysis.

Discussion

GSA-RhodG is a promising molecular imaging agent for detecting tiny ovarian cancer implants in the peritoneal cavity due to its bright emission and relatively rapid clearance from the peritoneal space within 3 h.[19,20] We have developed a similar but activatable and sprayable fluorescent probe based on the RhodG platform as well.[21] However, we found that these RhodG-based probes did not work as well in mice with bloody ascites due to diminished fluorescence. The results of the present study demonstrate that FLTI is superior to fluorescence imaging in detecting tumors partly covered with bloody ascites. The FLTI allowed detection of tumors on the peritoneal surface, even when conventional fluorescence imaging was markedly constrained by the presence of bloody ascites. However, full-field FLTI is probably not practical at this time as it would take several minutes to acquire and would be degraded by bowel and organ motion. However, a single-pixel

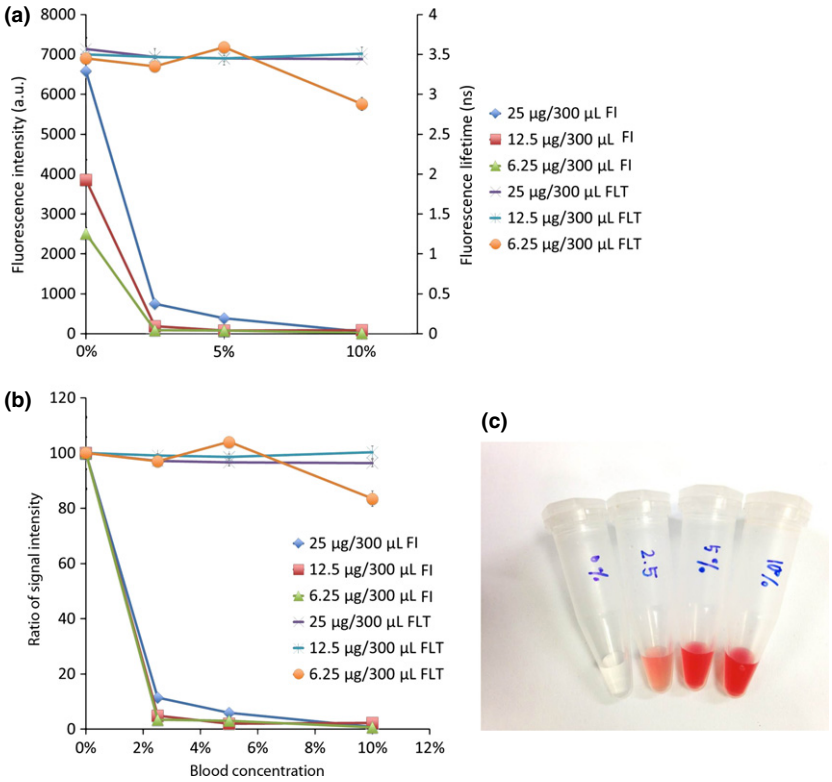

Fig. 4. Effect of blood on the fluorescence intensity and fluorescence lifetime for galactosyl serum albumin-rhodamine green (GSA-RhodG) solution. Mouse blood was added to the GSA-RhodG solution at a concentration of 21, 41 and 83 μg/mL. The final blood ratios were adjusted to 2.5%, 5% and 10%. (a) Comparison between the fluorescence intensities and lifetimes for GSA-RhodG solution with or without blood. The fluorescence intensities were decreased in an inverse proportion to the addition of blood. The fluorescence lifetime values were almost the same at all blood ratios. (b) The ratio of the fluorescence intensities and lifetimes of blood + GSA-RhodG compared with the baseline GSA-RhodG solution. Fluorescence intensities were dramatically decreased to <10% after adding only 2.5% blood, whereas the fluorescence lifetime values were almost the same at any blood ratio. (c) White light image for samples of GSA-RhodG with and without added blood at concentrations of 0, 2.5%, 5% and 10%.

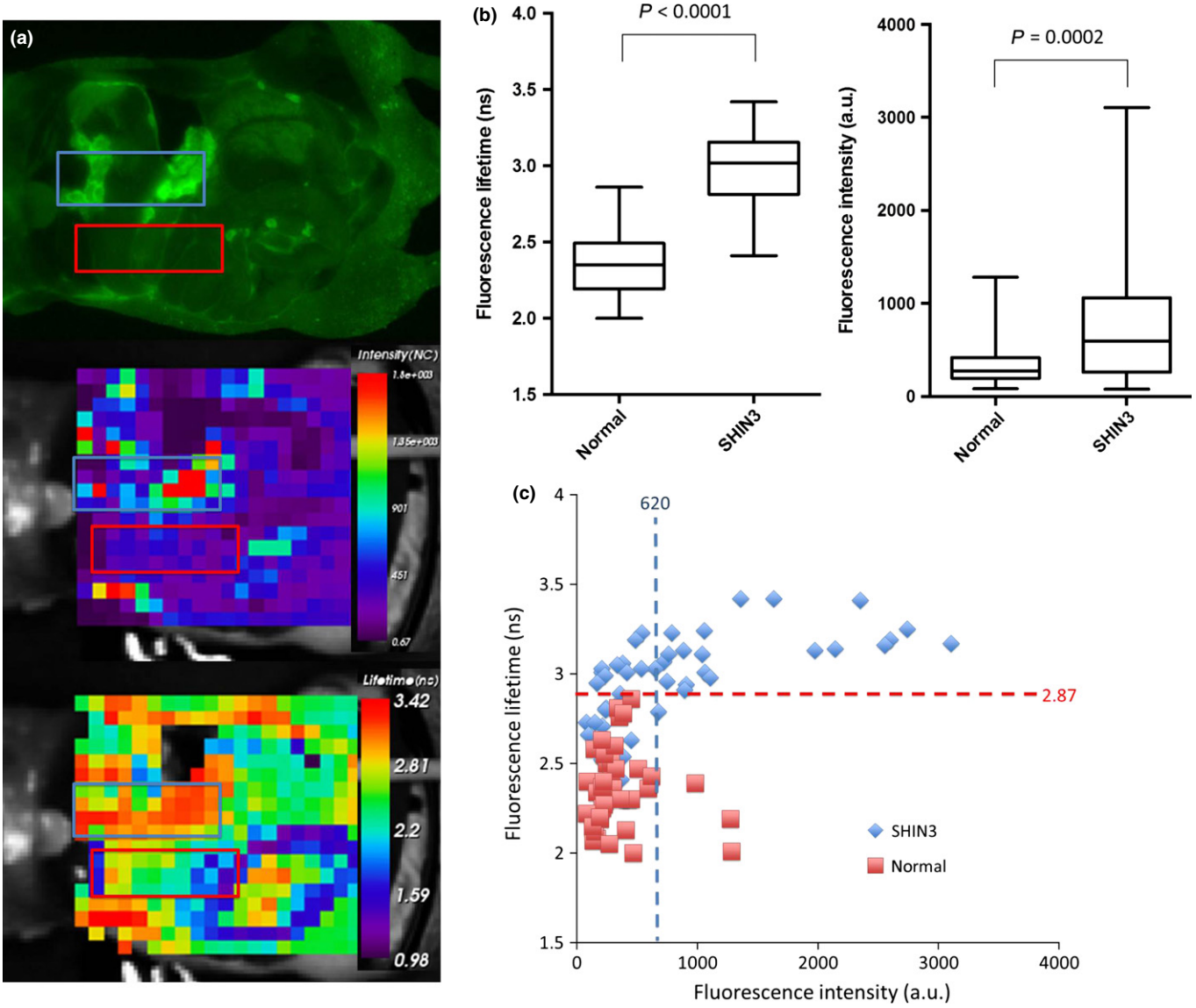

Fig. 5. *In vivo* fluorescence intensities and fluorescence-lifetime images of tumor-bearing mice without ascites. (a) Fluorescence images on Maestro (upper) and OPTIX-MX2 (middle) and a fluorescence-lifetime image (lower). The blue and red rectangles on *in vivo* images were selected as an objective area for voxel by voxel comparison between the fluorescence intensities and lifetimes. The blue rectangles on these images define regions containing SHIN3 tumors, whereas the red rectangles encompass normal tissue only. (b) Box plots comparing fluorescence lifetime values and fluorescence intensities between normal tissue and tissue containing tumors. (c) Every pixel in each rectangle was plotted to allow a "dot by dot" comparison of fluorescence intensities and fluorescence lifetime values.

FLT measurement could be acquired in approximately 10 ms and therefore a long FLT in a single region of interest might alert a clinician that a tumor implant might lay hidden under bloody fluid during a procedure.

The FLT of GSA-RhodG is much longer (3.3–3.5 ns) than the FLT of autofluorescence in the green range, which is typically <1.8 ns, mostly dependent on the presence of collagen. Because of this marked difference between FLT of the target and that of the background, FLTI can overcome some of the limitations with attenuation of detectable fluorescence due to ascites.

The FLTI remains independent of the concentration of dye as long as the fluorescence signal can be detected. In our GSA-RhodG solution study with blood, the addition of only 2.5% blood to the fluid markedly decreased fluorescence intensities below 10% of baseline. The addition of 10% blood decreased the fluorescence signal to <1%, demonstrating a strong susceptibility of fluorescence intensity to the presence of blood in the surrounding fluid. This finding can be traced to the fact that RhodG has an absorption peak at 503 nm and a emission peak at 527 nm. Red blood cells have a broad absorption band at visible light (approximately 300–650 nm). Therefore, both the excitation and emission light for GSA-RhodG are dramatically reduced in the presence of bloody ascites.

A potential alternative to FLTI is the use of fluorescent proteins including green and red fluorescent proteins, which are excellent endogenous fluorescence emitters to be used for depicting various biological processes both *in vitro* and *in vivo*.[22,23] A recently reported alternative technology to this method is tumor-specific imaging using telomerase promoter-regulated expression of fluorescent proteins, which are induced with

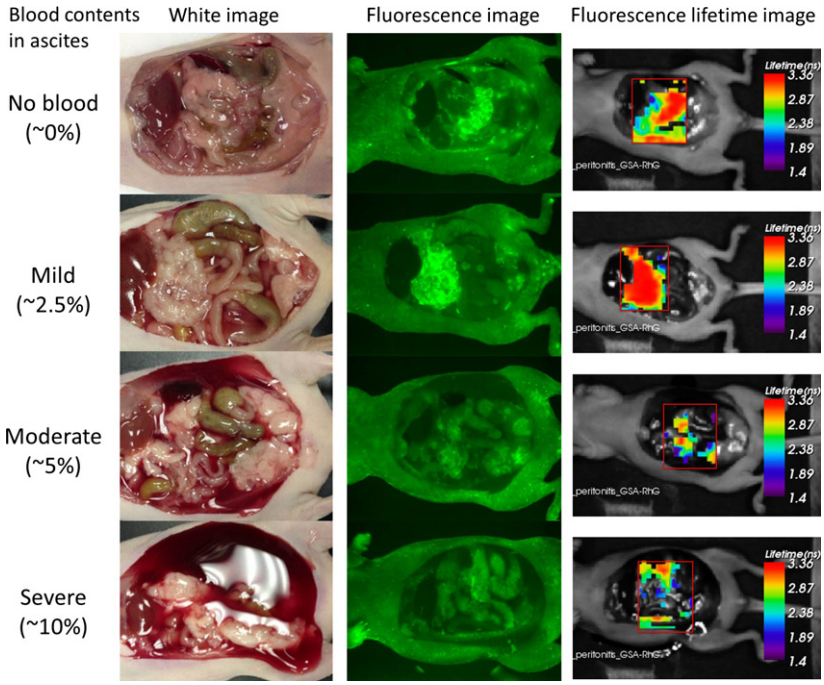

Fig. 6. *In vivo* fluorescence intensities and fluorescence-lifetime images of tumor-bearing mice with various grades of bloody ascites. Hemorrhagic ascites in peritoneal ovarian cancer mice varied from no blood (~0%) to severe (~10% blood). Identifying tumors in moderate to severe hemorrhagic ascites was difficult using conventional fluorescence imaging due to absorption by hemoglobin; however, fluorescence-lifetime imaging readily demonstrated the tumors at all degrees of bloody ascites.

adenovirus-mediated gene transfection *in vivo*.[24,25] Green fluorescent protein (GFP) and red fluorescent protein (RFP) reportedly show FLT of approximately 2.8 and 2.4 ns, respectively,[26] which is sufficiently longer than FLT of autofluorescence, but shorter than RhodG used in the present study. Therefore, the method of FLTI described here can be used with GFP and RFP; however, the difference of FLT between GFP and autofluorescence would be smaller and therefore more difficult to discern. However, endogenous proteins such as GFP are limited because they require virus-mediated *in vivo* gene transfection, which is unlikely to be permitted in humans, at least in the near term.

In the present study we used a model of ovarian cancer peritoneal implants with hemorrhagic ascites. In clinical practice, such ascites might be easily washed away. However, during surgical removal of lesions it is common for bleeding to occur and mix with fluids used to wash the peritoneum leading to pooling of fluid in recesses that could harbor tumors. As surgeons adopt laparoscopic procedures to reduce the invasiveness of surgery, the problem of identifying tumors with areas of pooled hemorrhagic fluid becomes even greater. Recently, the FDA approved intraoperative surgical cameras for fluorescence-guided navigation surgery but, to date, these have depended on conventional fluorescence imaging. Our work shows that the next generation of such cameras might benefit from including FLTI or even single-pixel FLT measurements to allow surgeons to scan regions that are concealed by pooled ascites. This could reduce the number of false-negative tumors and improve the overall outcomes from debulking surgery.

In conclusion, FLTI with GSA-RhodG depicted ovarian cancer lesions that were invisible on conventional fluorescence imaging due to the presence of hemorrhagic ascites. This work indicates that adding FLTI to conventional intraoperative fluorescence cameras might extend the value of such devices for detecting small tumors during surgeries in which pooled hemorrhagic fluid/ascites are likely to occur.

Acknowledgment

This research was supported by the Intramural Research Program of the National Institutes of Health, National Cancer Institute, Center for Cancer Research.

Disclosure Statement

The authors have no conflict of interest.

References

1 Frangioni JV. New technologies for human cancer imaging. *J Clin Oncol* 2008; **26**: 4012–21.
2 Kim S, Lim YT, Soltesz EG *et al.* Near-infrared fluorescent type II quantum dots for sentinel lymph node mapping. *Nat Biotechnol* 2004; **22**: 93–7.
3 Tanaka E, Choi HS, Fujii H, Bawendi MG, Frangioni JV. Image-guided oncologic surgery using invisible light: completed pre-clinical development for sentinel lymph node mapping. *Ann Surg Oncol* 2006; **13**: 1671–81.
4 Akyürek M, Şafek T, Sönmez E, Özkan Ö, Keçik A. A new flap design: neural-island flap. *Plast Reconstr Surg* 2004; **114**: 1467–77.
5 Alkureishi LWT, Shaw-Dunn J, Ross GL. Effects of thinning the anterolateral thigh flap on the blood supply to the skin. *Br J Plast Surg* 2003; **56**: 401–8.
6 Holm C, Mayr M, Höfter E, Becker A, Pfeiffer UJ, Mühlbauer W. Intraoperative evaluation of skin-flap viability using laser-induced fluorescence of indocyanine green. *Br J Plast Surg* 2002; **55**: 635–44.
7 Langer S, Biberthaler P, Harris AG, Steinau HU, Messmer K. *In vivo* monitoring of microvessels in skin flaps: introduction of a novel technique. *Microsurgery* 2001; **21**: 317–24.
8 Mothes H, Dönicke T, Friedel R, Simon M, Markgraf E, Bach O. Indocyanine-green fluorescence video angiography used clinically to evaluate tissue perfusion in microsurgery. *J Trauma* 2004; **57**: 1018–24.
9 Longmire MR, Ogawa M, Hama Y *et al.* Determination of optimal rhodamine fluorophore for *in vivo* optical imaging. *Bioconjug Chem* 2008; **19**: 1735–42.
10 Proulx ST, Luciani P, Alitalo A *et al.* Non-invasive dynamic near-infrared imaging and quantification of vascular leakage *in vivo*. *Angiogenesis* 2013; **16**: 525–40.

11 Berezin MY, Achilefu S. Fluorescence lifetime measurements and biological imaging. *Chem Rev* 2010; **110**: 2641–84.
12 Bloch S, Lesage F, McIntosh L, Gandjbakhche A, Liang K, Achilefu S. Whole-body fluorescence lifetime imaging of a tumor-targeted near-infrared molecular probe in mice. *J Biomed Opt* 2005; **10**: 054003.
13 Hassan M, Riley J, Chernomordik V *et al.* Fluorescence lifetime imaging system for *in vivo* studies. *Molecular imaging* 2007; **6**: 229–36.
14 Kobayashi H, Ogawa M, Alford R, Choyke PL, Urano Y. New strategies for fluorescent probe design in medical diagnostic imaging. *Chem Rev* 2010; **110**: 2620–40.
15 Bastiaens PI, Squire A. Fluorescence lifetime imaging microscopy: spatial resolution of biochemical processes in the cell. *Trends Cell Biol* 1999; **9**: 48–52.
16 Suhling K, French PMW, Phillips D. Time-resolved fluorescence microscopy. *Photochem Photobiol Sci* 2005; **4**: 13–22.
17 Wallrabe H, Periasamy A. Imaging protein molecules using FRET and FLIM microscopy. *Curr Opin Biotechnol* 2005; **16**: 19–27.
18 Regino CAS, Ogawa M, Alford R *et al.* Two-step synthesis of galactosylated human serum albumin as a targeted optical imaging agent for peritoneal carcinomatosis. *J Med Chem* 2010; **53**: 1579–86.
19 Gunn AJ, Hama Y, Koyama Y, Kohn EC, Choyke PL, Kobayashi H. Targeted optical fluorescence imaging of human ovarian adenocarcinoma using a galactosyl serum albumin-conjugated fluorophore. *Cancer Sci* 2007; **98**: 1727–33.
20 Hama Y, Urano Y, Koyama Y, Bernardo M, Choyke PL, Kobayashi H. A comparison of the emission efficiency of four common green fluorescence dyes after internalization into cancer cells. *Bioconjug Chem* 2006; **17**: 1426–31.
21 Urano Y, Sakabe M, Kosaka N *et al.* Rapid cancer detection by topically spraying a γ-glutamyltranspeptidase-activated fluorescent probe. *Sci Transl Med* 2011; **3**: 110ra9.
22 Kishimoto H, Aki R, Urata Y *et al.* Tumor-selective, adenoviral-mediated GFP genetic labeling of human cancer in the live mouse reports future recurrence after resection. *Cell Cycle* 2011; **10**: 2737–41.
23 Kishimoto H, Urata Y, Tanaka N, Fujiwara T, Hoffman RM. Selective metastatic tumor labeling with green fluorescent protein and killing by systemic administration of telomerase-dependent adenoviruses. *Mol Cancer Ther* 2009; **8**: 3001–8.
24 Bouvet M, Hoffman RM. Glowing tumors make for better detection and resection. *Sci Transl Med* 2011; **3**: 110 fs10.
25 Kishimoto H, Zhao M, Hayashi K *et al. In vivo* internal tumor illumination by telomerase-dependent adenoviral GFP for precise surgical navigation. *Proc Natl Acad Sci USA* 2009; **106**: 14514–7.
26 Jakobs S, Subramaniam V, Schonle A, Jovin TM, Hell SW. EGFP and DsRed expressing cultures of *Escherichia coli* imaged by confocal, two-photon and fluorescence lifetime microscopy. *FEBS Lett* 2000; **479**: 131–5.